Polylactic Acid/Ethylene Glycol Triblock Copolymer as Novel Crosslinker for Epoxidized Natural Rubber

T.-H. Nguyen,[1] P. Tangboriboonrat,[2] N. Rattanasom,[3] A. Petchsuk,[4] M. Opaprakasit,[5] C. Thammawong,[1] P. Opaprakasit[1]

[1]*School of Bio-Chemical Engineering and Technology, Sirindhorn International Institute of Technology (SIIT), Thammasat University, Pathum Thani 12121, Thailand*
[2]*Department of Chemistry, Faculty of Science, Mahidol University, Phyathai, Bangkok 10400, Thailand*
[3]*Institute of Molecular Biosciences, Mahidol University, Salaya, Nakhon Pathom 73170, Thailand*
[4]*Polymer Research Unit, National Metal and Materials Technology Center (MTEC), National Science and Technology Development Agency, Pathum Thani 12120, Thailand*
[5]*Department of Materials Science, Faculty of Science, Center for Petroleum, Petrochemicals and Advanced Materials, Chulalongkorn University, Bangkok 10330, Thailand*

Received 24 September 2010; accepted 13 June 2011
DOI 10.1002/app.35088
Published online 3 October 2011 in Wiley Online Library (wileyonlinelibrary.com).

ABSTRACT: Polylactic acid/ethylene glycol triblock copolymer ($LLA_{46}EG_{46}LLA_{46}$) was prepared and used in a crosslink process of epoxidized natural rubber (ENR) by employing a ring-opening reaction using $Sn(Oct)_2$ as a catalyst. The OH-capped copolymer acts as a macromolecular crosslinking agent in the formation of ENR networks, leading to drastic enhancement in tensile properties. Crosslink efficiency and chemical structures of the cured materials are examined by solvent fractionation, swelling experiments, XRD, ^{1}H-NMR, and ATR-FTIR spectroscopy. The efficiency of the curing process is dependent on the ENR/copolymer feed ratios. The degree of property improvement and gas permeability/selectivity behaviors of the cured materials are strongly dependent on the copolymer content and the efficiency of the curing process.
 J Appl Polym Sci 124: 164–174, 2012

Key words: rubber; crosslinking; gas permeation; biodegradable; block copolymers

INTRODUCTION

Natural rubber (NR) is known as a "green," sustainable, renewable, and biodegradable material.[1] However, NR latex film cannot be used without vulcanization because it is not very strong and lacks elasticity. Vulcanization is required to introduce chemical network junctures between rubber or polyisoprene chains to form crosslinked networks, which enhances their mechanical properties suitable for applications. Vulcanization is mainly classified as sulfur and nonsulfur processes. The crosslink junctures from sulfur vulcanization are derived from either single sulfur atoms or short-chain sulfur compounds with accelerators such as 2-benzothiazole disulfide.[2–4] In contrast, organic peroxides for example dicumyl peroxide[5–8] are commonly used in non-sulfur vulcanization. In addition, NR latex can be vulcanized by employing chemical-free processes, such as using electron beam,[9] γ ray,[10,11] UV radiation, and ultrasonic wave.[12]

Vulcanization by crosslinking of specially functionalized rubbers has attracted great interest in the research community. Epoxide groups are introduced and used as crosslink sites instead of allylic groups in sulfur vulcanization.[12–14] The double bonds of NR are well known to react with peracids to produce epoxide groups in the conversion of NR to epoxidized NR (ENR). This process leads to an enhancement in certain properties, such as higher hysteresis and oil resistance, and lower air permeability compared with its native NR counterpart.[13,15] Moreover, epoxide groups can readily react with many nucleophilic reagents for further modification of the material properties, such as amines,[14,16,17] phosphorus,[18] and carboxylic acids.[19] The interest of reacting hydroxyl groups with ENR has been initiated and reported by Derouet et al., where alcohols were grafted onto ENR backbone through ring-opening reaction of its epoxide.[20,21]

Polylactic acid (PLA) is a biodegradable/biocompatible polymer that is particularly attractive for use in various applications, especially in biomedical fields.[22] However, its low hydrophilicity limits its use in certain applications. Therefore, poly(ethylene

Correspondence to: P. Opaprakasit (pakorn@siit.tu.ac.th).
Contract grant sponsor: The Thailand Research Fund/Office of Higher Education Commission; contract grant number: RTA5180003.
Contract grant sponsors: National Research University Project of Thailand Office of Higher Education Commission, Thailand Toray Science Foundation, Siam Cement Foundation and SIIT, Thammasat University.

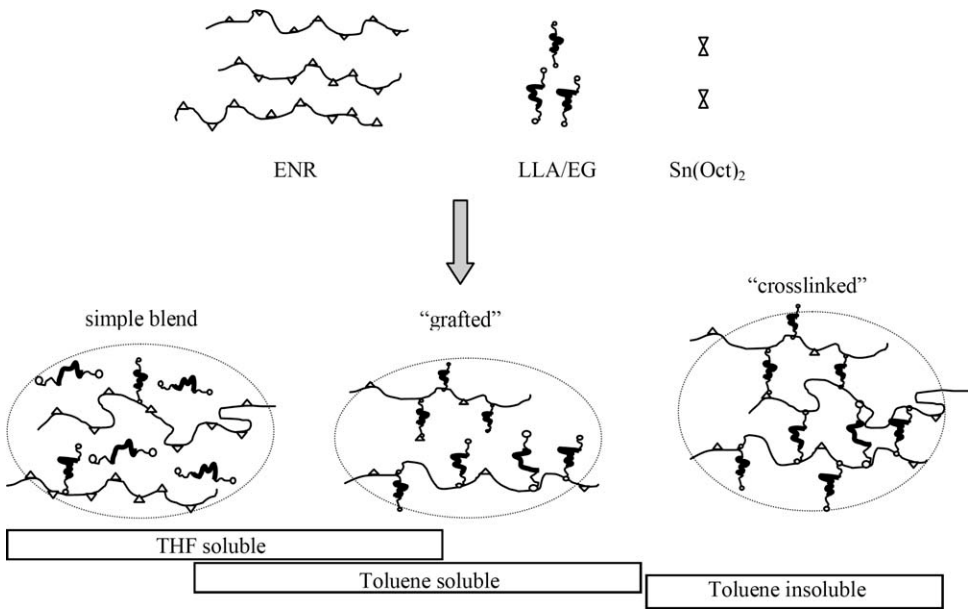

Figure 1 Proposed curing reaction of ENR by OH-capped LLA/EG/LLA block copolymer, and the possible structures of the "cured" products and their solvent solubility.

glycol) (PEG), a hydrophilic polymer with outstanding properties, i.e., nontoxicity and biocompatible characteristics, is introduced. Copolymerization of PLA and PEG at various compositions offers an opportunity to combine the advantages of these polymers to obtain biocompatible/degradable materials with tailored hydrophilicity.[23–25] Incorporation of NR with PLA has been conducted to improve its mechanical properties, especially the impact strength. It was reported that miscibility enhancement of ENR/PLA blend was achieved by a reactive mixing process at high temperature. The reaction of epoxides of ENR and ester groups of PLA was proposed as the origin of this enhancement.[26,27]

In our previous work,[28] OH-capped triblock copolymers of L-lactide (LLA) and ethylene glycol (EG) were synthesized by ring-opening polymerization of LLA using PEG as a macroinitiator. The LLA/EG/LLA copolymers with various block lengths and hence different properties were prepared by varying LLA/PEG molar ratios. In this study, the block copolymer is used as macromolecular crosslinker for ENR by utilizing the reaction of its two hydroxyl groups at the chain-ends with epoxides of ENR.[20,21] Properties of the resulting cured ENR products are then characterized. The materials are not only biocompatible and biodegradable, but also exhibit good mechanical properties comparable to conventionally cured rubber materials. Gas permeability behaviors of the cured ENR are also characterized for potential use in high-value and specific applications: membranes or medical applications such as breathable gloves or patches. Most importantly, the properties of these materials can be further modified by varying block lengths of the copolymer, epoxide content of ENR, and the copolymer/ENR feed ratios for specific applications.

EXPERIMENTAL

Materials

OH-capped $LLA_{46}EG_{46}LLA_{46}$ triblock copolymer was synthesized by the method reported in our previous work.[28] ENR with 20% epoxidation (ENR20) was synthesized from commercial high ammonia (HA)-preserved NR latex concentrate (Rayong Bangkok Rubber, Thailand) based on the methodology reported by Saendee et al.[29] $Sn(Oct)_2$ (Wako) and dried tetrahydrofuran (THF) was respectively, used as a catalyst and solvent.

Crosslinking of ENR by LLA/EG copolymer

The crosslink reaction was conducted by mixing ENR20 and the OH-capped $LLA_{46}EG_{46}LLA_{46}$ copolymer at three weight compositions (4/1, 2/1, 1/1) in dried THF (20% w/v) at 50°C. The samples are referred to as R41, R21, and R11, respectively. The mixture solution was first dried under vacuum for 1 h before purging with nitrogen gas. $Sn(Oct)_2$ catalyst (1 wt % of copolymer) was then added. The crosslink reaction was performed in a round-bottom flask equipped with magnetic stirrer at 70°C for 24 h.

The proposed chemical structures of the cured ENR products obtained from the reaction with the OH-capped copolymer are illustrated in Figure 1. When both OH end groups of the copolymer

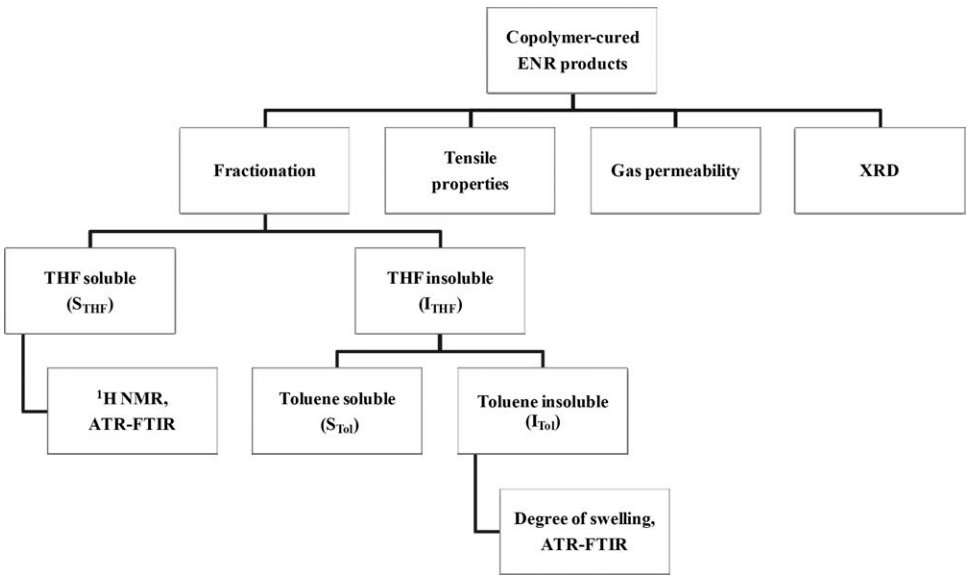

Figure 2 Overview of characterizations of the copolymer-cured ENR products.

undergo ring-opening reaction with epoxides of ENR, crosslink junctions are generated. In contrast, grafting of copolymer onto ENR backbone is achieved when only one hydroxyl per copolymer chain reacts. As ENR20 has 20% epoxide content, grafted ENR products with varied degree of grafting are generated. Additionally, unreacted copolymer chains may be present in the ENR matrix as a blended mixture, due to an excess amount of copolymer, when ENR20/copolymer ratios are varied. These possibilities will be referred to as "crosslinked," "grafted," and "free" or simple blend fractions. These fractions of products exhibit different solubility behaviors (discussed later), as summarized in Figure 1.

Characterizations

The cured ENR product, suspended in THF solvent after the crosslink reaction, was cast on a Teflon plate at room temperature. After completion of solvent evaporation, film samples ($\sim$ 0.1 mm thick) were obtained. The samples were then characterized as summarized in Figure 2. First, efficiency of the curing process in terms of weight fraction of "crosslinked," "grafted," and "free" copolymers in ENR matrix, was examined by sequential solvent fractionation, employing THF and toluene solvents. Given that ENR and the copolymer are completely dissolved in THF at 50°C, Soxhlet extraction by THF was first employed for 24 h to determine the weight content of remaining uncured ENR and "free" or unreacted copolymers in the soluble fraction (denoted by S_{THF}), which was recovered by complete evaporation of the solvent. The THF-insoluble fraction (I_{THF}) was then further extracted by toluene at room temperature for seven days. The soluble and insoluble fractions (denoted by S_{Tol} and I_{Tol}), corresponding to "grafted" and fully "crosslinked" ENR domains, respectively, were recovered. The remaining weight of each fraction was then recorded and the weight percentage was calculated based on mass of the original sample. Chemical structures and chain compositions of each fraction were characterized by ^{1}H-NMR spectroscopy on a Bruker DRX400 using $CDCl_3$ as a solvent. ATR-FTIR spectra of each fraction were recorded on a ThermoNicolet 6700 model spectrometer. The spectra were recorded at 2 cm^{-1} resolution with 32 scans. ATR accessory equipped with ZnSe with a face angle of 45° was employed.

The crosslink density of the toluene insoluble (I_{Tol}) samples was examined by using the solvent swelling method. A piece of sample was accurately weighed and then immersed in toluene (40 mL) at room temperature in a dark cabinet. At equilibrium swelling time, where a constant solvent weight uptake was reached (about seven days), the test piece was removed, wiped with filter paper, and its weight was recorded. The swelling percentage was calculated, as follows:

$$\%\,\text{swelling} = \frac{W_{eq} - W_o}{W_o} \times 100 \qquad (1)$$

where W_o = original weight of dried sample (g)

W_{eq} = weight of swollen sample at equilibrium swelling time (g)

Tensile tests were carried out using dumbbell specimens cut from the cured rubber films (prepared from solution cast technique) with a thickness of $\sim$ 0.1 mm by using the Type II die, in accordance with ISO 37. At the onset of testing, two extensometer clamps were set and attached to the sample 20-mm apart within the gauge region. The cross-head

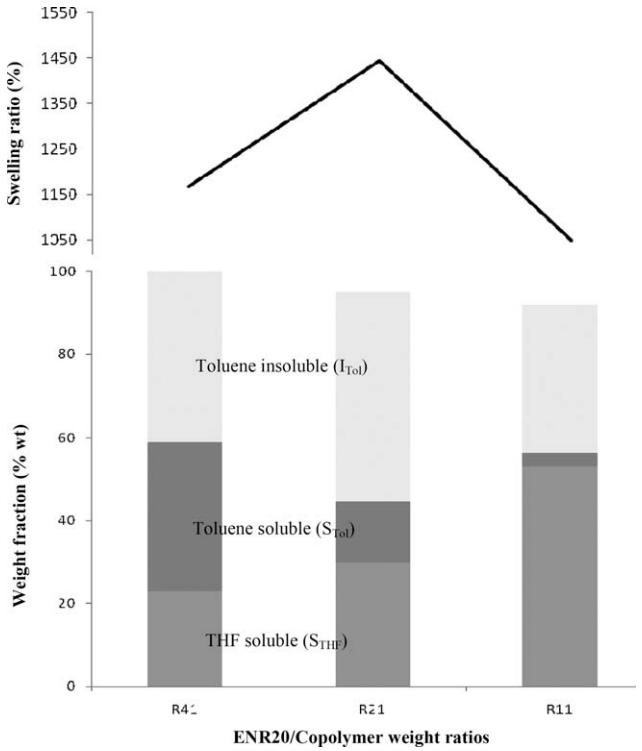

Figure 3 Solvent extraction results and swelling behaviors of cured products as a function of ENR20/copolymer feed content.

speed and full scale force used were 100 mm/min and 1 kN, respectively. The specimens were pulled in tension until rupture. The values of 100 and 300% modulus, tensile strength, and elongation at break were recorded, and the average value from three to four specimens was reported. Crystalline characteristics of the cured samples were examined by XRD on a JEOL JDX-3530 Diffractometer, using $CuK_{\alpha 1}$ radiation. The sample films were scanned from 2θ of 5–40° with 0.02 step size.

Permeability tests were also conducted on cast film samples with thickness of ~ 0.1 mm. Water vapor permeability was measured on an Illinois instrument (Model 7200), using ASTM F1249-01 at 38°C, 90% relative humidity and 1 atm pressure. Oxygen permeability was recorded on a Mocon instrument (Ox-Tran Model 2/21), following ASTM D3985 at 23°C, 0% relative humidity. Carbon dioxide permeability was measured on a Mocon instrument (Permatran-C Model 4/41) at 23°C, 0% relative humidity.

RESULTS AND DISCUSSION

Solvent fractionation

Results on weight percentage of products obtained from sequential solvent fractionation are summarized in Figure 3. As ENR20, LLA/EG copolymer, and a simple mixture of the two materials are completely dissolved in THF at 50°C, the content of S_{THF}, therefore, indicates the amount of the "free" or simple blend fraction. It is noted that slightly grafted ENR chains (copolymer-grafted ENR with low degree grafting) are also extractable by THF.[30,31] This is confirmed by NMR spectrum of the soluble material, where peaks due to copolymer dominate, with weak signals associated with ENR, as shown in Figure 4.

The content of the insoluble extracted sample (I_{THF}) represents the amount of newly formed "crosslinked" structure and "grafted" ENR domains, which are not soluble in THF solvent.[30,31] These two fractions are then further separated by toluene extraction. The "grafted" portions are soluble in toluene, while the "crosslinked" network remains insoluble. Unlike its slightly grafted counterpart, solubility behavior of the "grafted" ENR in toluene (but not THF) may be explained in terms of a decrease in epoxide content of ENR as a result of conversion to grafting points, and a large increase in the molecular weight of the "grafted" products. These two effects lead to a decrease in polarity and hence lower solubility in THF.

In the sample with low copolymer content in feed (R41), "crosslinked" and "grafted" fractions of ~ 40 and 36 wt % are observed. Unreacted "simple blend" of ~ 20 wt % is obtained. These indicate that the majority of hydroxyl groups in the copolymer chains effectively react with ENR20. When the copolymer content in feed is increased, the weight content of the "crosslinked" fraction is significantly comparable in all samples at ~ 40 wt %. In contrast, those of the "grafted" and the "simple blend" portions vary with the copolymer content. The "simple blend" (S_{THF}) content increases with an increase in the copolymer content in feed, while that of the "grafted" (S_{Tol}) fraction shows the opposite trend. Therefore, the feed ratio of ENR20/copolymer can be optimized to control the reaction efficiency. It is noted that the ENR : copolymer weight ratios of 4 : 1, 2 : 1, and 1 : 1 are equivalent to epoxide : OH molar ratios of 50 : 1, 25 : 1, and 12 : 1, respectively. The variation in the feed ratio leads to changes in two factors, i.e., the probability of copolymer's hydroxyls reacting with ENR (grafting efficiency), and the crosslinking efficiency (two hydroxyls from the same copolymer chain react with ENR to form crosslink junctions).

The increase in hydroxyls content leads to an increase in the grafting efficiency, which may reach a constant value when the limiting reagent (hydroxyl) is completely consumed. It was expected that hydroxyl groups are completely consumed in all three compositions. However, it is observed that unreacted copolymer remain in all samples even in

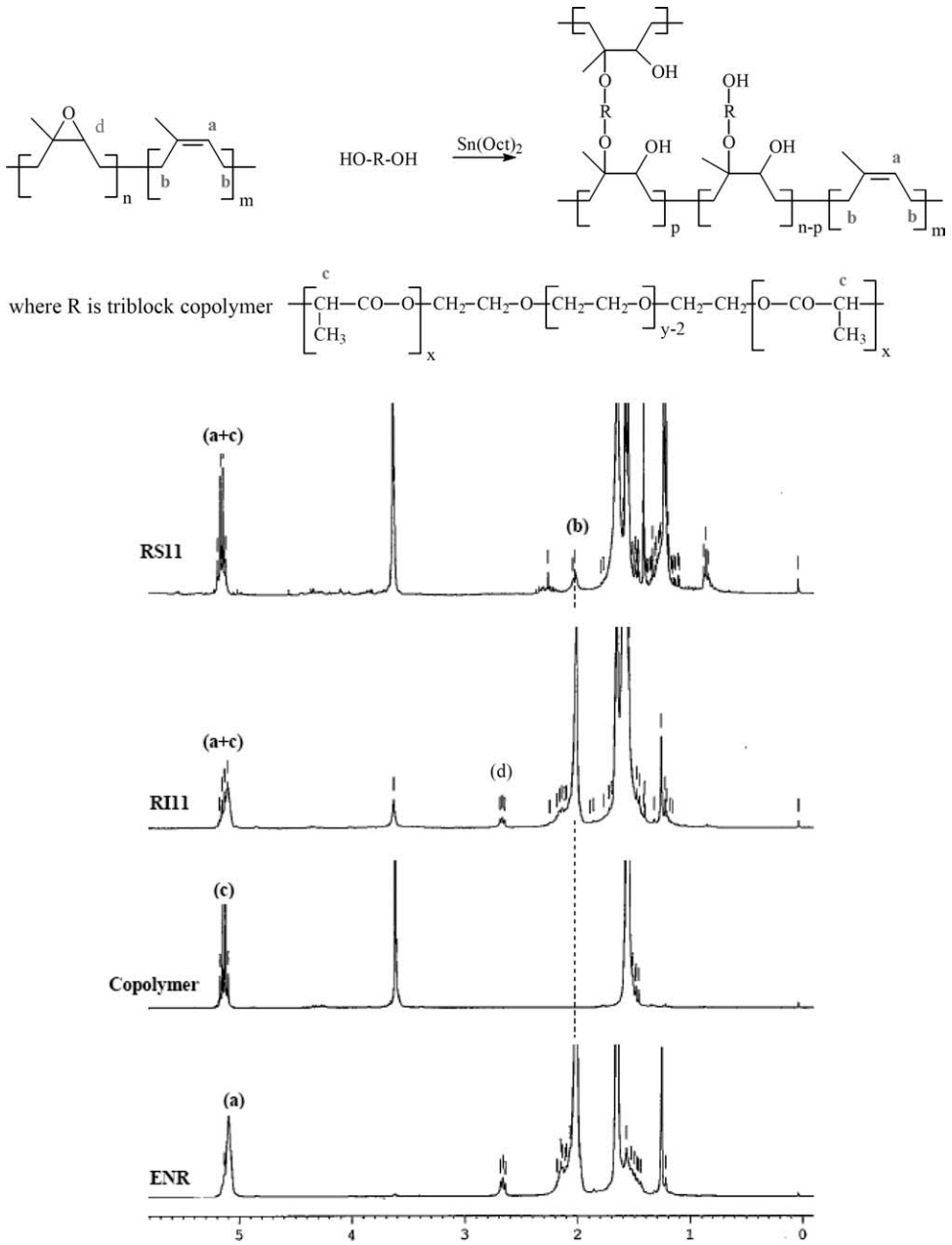

Figure 4 ^{1}H-NMR spectra and signal assignments of ENR20, $LLA_{46}EG_{46}LLA_{46}$ triblock copolymer, insoluble (I_{THF}11) and soluble (S_{THF} 11) fractions of the cured products after THF Soxhlet extraction.

the sample with the epoxide : hydroxyl molar ratio as high as 50 : 1. This is probably due to restriction in accessibility of the hydroxyls to epoxides, i.e., epoxide groups are spaced apart in ENR chains (20% epoxidation). In addition, steric factors and chain stiffness also play a role, as the hydroxyls are terminal groups of long copolymer chains and ENR contains double bonds in its backbone. Nonetheless, improvement of the grafting efficiency can be achieved by employing a reactive blend process, where catalyst and mechanical force are applied to aid the reaction. This will be reported in a separate communication.

In contrast, the increase in the feed hydroxyl content leads to a lower probability for two hydroxyl end-groups from the same copolymer chain, to react and form crosslink junctions, compared with that of forming grafted points. This results in a decrease in the crosslink efficiency. Figure 3 clearly indicates that the content of "grafted" fraction decreases upon increasing the feed ratio from 4 : 1 to 1 : 1. This reflects that the former effect is a dominant factor in this curing process. It is noted that solubility behavior of copolymer-grafted ENR chains varies with the degree of grafting. This may cause some uncertainties in the results obtained from the sequential

solvent extraction, as "grafted" ENR with certain range of degree of grafting is likely to dissolve in both THF and toluene solvents, as indicated by an overlap area of solubility in Figure 1.

Degree of crosslinking

Degree of crosslinking of the insoluble fraction after solvent fractionation (I_{Tol}) is examined in terms of the swelling percentage in toluene. The results are also summarized in Figure 3. All samples exhibit a swelling ability, higher than 10 times their original dimensions, where the lowest swelling ratio of 1050% is observed in the sample derived from a 1 : 1 ENR20/copolymer feed ratio, indicating the highest crosslink density. This value is clearly higher ($\sim$ 2-fold) than those reported for typical sulfur-vulcanized NR samples,[32] where short sequences of sulfur bridges are employed as crosslink junctions. These results firmly support our proposed crosslink mechanism and structures that the copolymers act as long-chain junctions, which provide higher flexibility for the rubber network swelling.

^{1}H-NMR spectra

Chemical structure of the cured ENR products is illustrated in Figure 4. Formation of "crosslinked" or "grafted" structures is obtained, as a result from the variation in ENR20/copolymer feed ratio. ^{1}H-NMR spectra and signal assignments of ENR20, $LLA_{46}EG_{46}LLA_{46}$ OH-capped triblock copolymer are also compared in Figure 4, where THF soluble and insoluble fractions of the R11 cured sample are also shown. Signals located near 5.10 ppm consist of a singlet of methine proton (a) of *cis*-1,4-isoprene repeat units and a quartet of methine proton (c) of lactate units. Signals located at 2.10 (b) and 2.65 (d) ppm are assigned to methylene proton of NR units and methine proton of ENR, respectively. The strong (b) signal and a combination of signals at 5.10 ppm (a+c) in the spectrum of the THF-insoluble fraction strongly indicate that the sample consists of ENR20 matrix with the presence of the copolymer as crosslinked junctions. In contrast, a weak (b) signal in the spectrum of the soluble fraction demonstrates that the sample mainly consists of "uncrosslinked" copolymers and some copolymer-grafted ENR.[26,33]

Content of the copolymer in the THF soluble fraction of the cured products is calculated from ^{1}H-NMR spectra, as follows:

$$S_c = S_{(a+c)} - S_a \quad (2)$$

S_a = peak integration of methine proton (5.10 ppm) of ENR

TABLE I
Weight Fractions and Copolymer Content of the Extracted Products After THF Soxhlet Extraction

Samples	ENR20/copolymer feed content (wt %)	Weight fraction[a] (wt %)	Copolymer content[b] (wt %)
$S_{THF}41$	75 : 25	23	63
$S_{THF}21$	66 : 33	30	84
$S_{THF}11$	50 : 50	53	90

[a] Result from Soxhlet extraction.
[b] Calculated from ^{1}H-NMR spectra.

S_c = peak integration of methine proton (5.10 ppm) of copolymer

S_{a+c} = peak integration of methine protons of ENR and copolymer

S_b = peak integration methylene proton (2.10 ppm) of *cis*-1,4-polyisoprene unit

The weight content of the copolymer in the samples is calculated, as follows:

$$C(\%) = \frac{M_P}{M_P + \left(S_b \times \frac{U_{LA}}{S_c} \times M_{NR}\right) \times \left(\frac{100}{100 - X_{epoxy}}\right)} \times 100 \quad (3)$$

where $C(\%)$ = weight content of the copolymer,

M_P = molar mass of copolymer (8600 g/mol),

U_{LA} = average number of LLA repeat units in the copolymer chain (92 units),

M_{NR} = molar mass of *cis*-1,4-polyisoprene repeat unit (68 g/mol),

X_{epoxy} = epoxide content of ENR20 (20%).

Results on the weight fraction and copolymer content of THF-soluble samples (S_{THF}), as summarized in Table I and Figure 3, show an increasing trend, as a function of increasing copolymer content in the feed. The increase in weight fraction of S_{THF} from the Soxhlet extraction reflects an increase in (excess) unreacted copolymers, present as simple blend component or small amount of "grafted" fraction with low degree of grafting. In addition, the increase in copolymer content of S_{THF} samples, calculated from NMR spectra, with the copolymer content in the feed also reflects that the S_{THF} sample consists of a certain amount of slightly grafted ENR and an increasing quantity of unreacted copolymers.

ATR-FTIR spectra

ATR-FTIR spectra of ENR20, LLA/EG copolymer, and R41 cured sample are shown in Figure 5. Characteristic bands of ENR20 are observed at 3030 (C—H stretching of epoxide), 1655 (C=C stretching of rubber unit), 1375 (C—H symmetric deformation of rubber's —CH_3), and 1250 cm^{-1} (C—O stretching

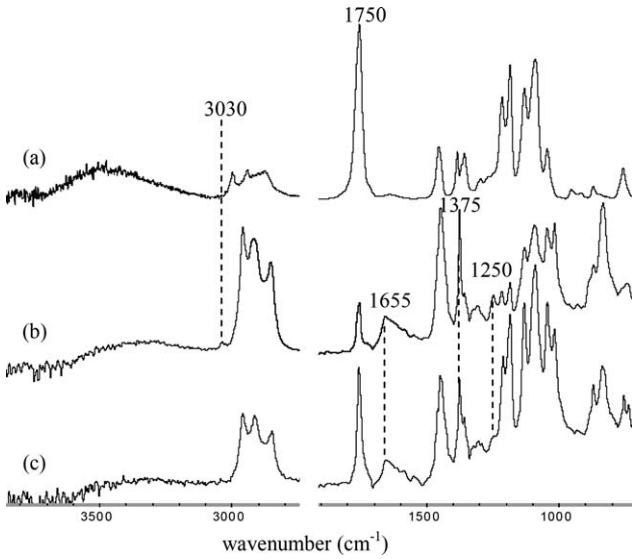

Figure 5 ATR-FTIR spectra of $LLA_{46}EG_{46}LLA_{46}$ triblock copolymer (a), ENR20 (b), and R41-cured sample (c).

of epoxide).[34] The characteristic absorption bands of LLA/EG triblock copolymer are observed at 1750 (C═O stretching), and 1375 and 1360 cm^{-1} (C—H symmetric deformation of —CH_3 of lactate).[34] The spectrum of R41 cured ENR sample, also shown in Figure 5, exhibits band characteristics of the two components. It is clearly observed that the epoxide bands located at 3030 and 1250 cm^{-1} decrease in band intensity upon reacting with the copolymers, indicating a reduction in epoxide content as a result from the ring-opening reaction with hydroxyl groups.

The infrared spectra of cured ENR samples prepared from different ENR20/copolymer feed ratios are compared in Figure 6. Changes in relative intensities of the band characteristics of the two components as a function of feed content are clearly observed. The relative quantity of the two components can be measured by examining the intensity ratio of the 1750/1655 or 1375/1360 cm^{-1} bands. The spectra indicate the intensity ratios that are in

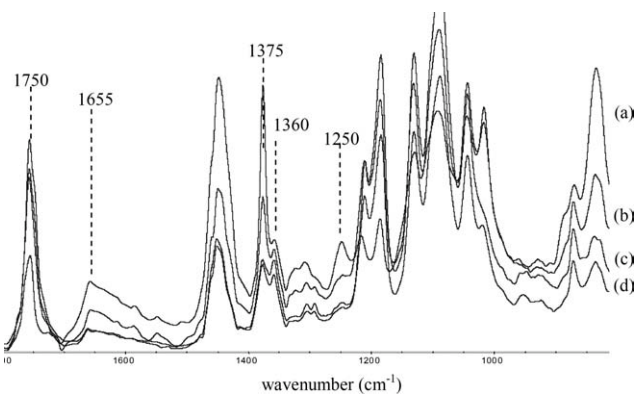

Figure 6 ATR-FTIR spectra of ENR20 (a), R41 (b), R21 (c), and R11 cured samples (d).

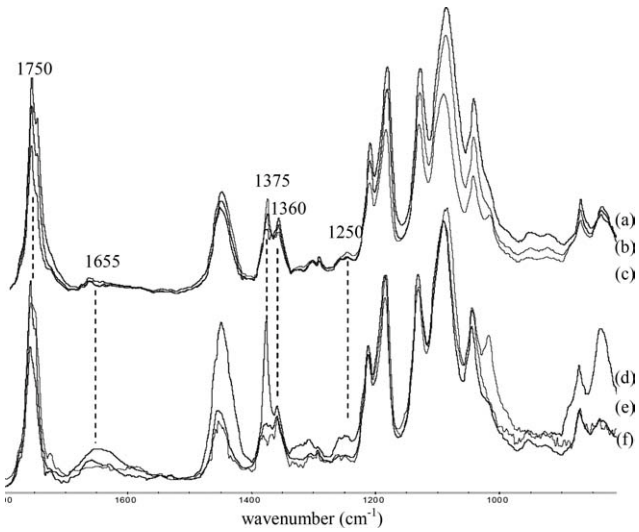

Figure 7 ATR-FTIR spectra of extracted products after THF Soxhlet extraction: $S_{THF}41$ (a), $S_{THF}21$ (b), and $S_{THF}11$ (c) soluble fractions; and $I_{THF}41$ (d), $I_{THF}21$ (e), and $I_{THF}11$ (f) insoluble fractions.

accord with the feed compositions. The efficiency of the curing process can be determined from the ATR-FTIR spectra by following the change in intensity of the 1250 cm^{-1} band, i.e., the epoxide content. The band intensity clearly decreases as the feed copolymer content increases, reflecting the conversion of epoxide groups after reaction with the hydroxyl groups. The corresponding spectra of THF extraction products, S_{THF} and I_{THF}, as a function of feed ENR20/copolymer content are compared in Figure 7. The change in relative intensity of band characteristics of the ENR and copolymer components is clearly observed, and the results are in accord with those observed from ^{1}H-NMR spectra.

XRD spectra

XRD traces of LLA/EG copolymer, ENR20 and the cured samples are compared in Figure 8. The spectrum of ENR20 shows a broad diffraction pattern due to its highly amorphous nature. In contrast, the spectrum of $LLA_{46}EG_{46}LLA_{46}$ copolymer show diffraction peaks at 2θ of 16.8, 19.1, and 22.4°, which correspond to crystalline domains of the LLA blocks. The diffraction patterns of EG blocks are not observed, probably because of its significantly short sequences and chain restriction imposed by the LLA terminal blocks that retards its crystallization. XRD traces of cured ENR products show diffraction peaks of the copolymer, whose intensity and sharpness increase with an increase in the copolymer content in the feed. This reflects an increase in the copolymer content in the cured products, and an enhancement in crystallize ability of the copolymer, due to excess amount of copolymer chains in the ENR

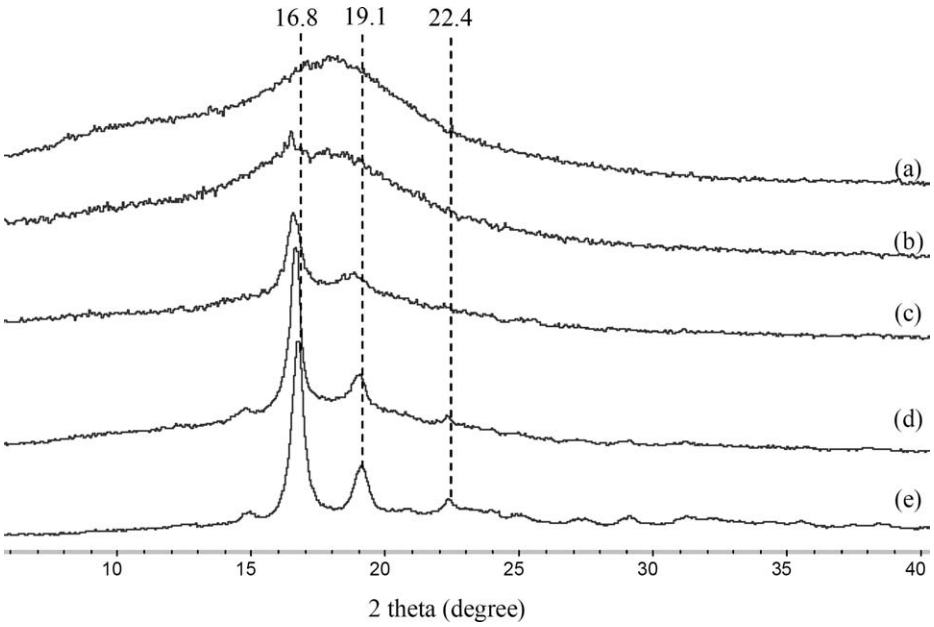

Figure 8 XRD traces of ENR20 (a), R41 (b), R21 (c), R11 (d) cured samples, and $LLA_{46}EG_{46}LLA_{46}$ triblock copolymer (e).

matrix. This is in good agreement with our previous discussion. It should also be noted that the peak position of the diffraction peaks, especially at 16.8°, shifts to lower angle along with the decrease in the peak intensity and sharpness as the feed ENR20/copolymer ratio increases from 1 : 1 to 4 : 1. This is probably due to lower degree of order arrangement of the copolymer domains, as the chains effectively react with the ENR and are present as "grafted" or "crosslink junctions." This results in mobility restriction, and hence a retardation of crystal formation.

Tensile properties

Tensile properties of R11 cured sample, a 1 : 1 ENR20/copolymer simple blended mixture without the use of catalyst (N11), and pristine ENR20 are examined and compared in Table II. It is noted that these samples do not contain ENR chains linked by conventional crosslinking junctions, i.e., reaction with double bonds. R11 and N11 show drastic improvement in 100% Modulus (M100), 300% Modulus (M300), and tensile strength, compared with those of the original ENR20. This indicates that the incorporation of LLA/EG copolymer, either by simple blending (N11) or as grafted chains and crosslink junctions (R11), leads to an enhancement in tensile properties of the samples. Given that the NMR spectrum of N11 and its extraction result (100% soluble in THF) indicate no significant chemical change in the simple blended mixture, the property improvement observed in this sample is probably attributed to interfacial adhesion of copolymer and ENR20 chains in the blend.[35] With the application of $Sn(Oct)_2$ catalyst, formation of "grafted" and "crosslinked" ENR networks by copolymer junctions is obtained in R11. This leads to further improvement in the tensile properties.

The elongation at break of R11 and N11 clearly decreases, compared to that of the original (uncured) ENR, because the incorporation of plastic materials, i.e., copolymers, into the rubber matrix leads to a decrease in elastic properties of the mixture, hence a drop in elongation at breaks. A mismatch in solubility parameter of the two components, which affects the mixture's miscibility, and the presence of excess copolymers may also play a role in the drop in the elongation at break of N11. The results also show that elongation at break of R11 is higher than that of N11. This is probably due to the existent of "grafted" ENR, which generate higher degree of chain entanglements and a closer match in solubility of the components, leading to an increase in elongation at break. In addition, the present of "crosslinked"

TABLE II
Tensile Properties of R11-Cured Sample, a 1 : 1 ENR20/Copolymer Blend (N11), and ENR20

Samples	M100 (MPa)	M300 (MPa)	Tensile strength (MPa)	Elongation at break (%)
R11	2.11 ± 0.10	3.98 ± 0.22	5.97 ± 0.31	407 ± 30
N11	1.88 ± 0.03	2.68 ± 0.04	3.14 ± 0.13	345 ± 25
ENR20	0.41 ± 0.02	0.42 ± 0.02	0.52 ± 0.04	650 ± 20

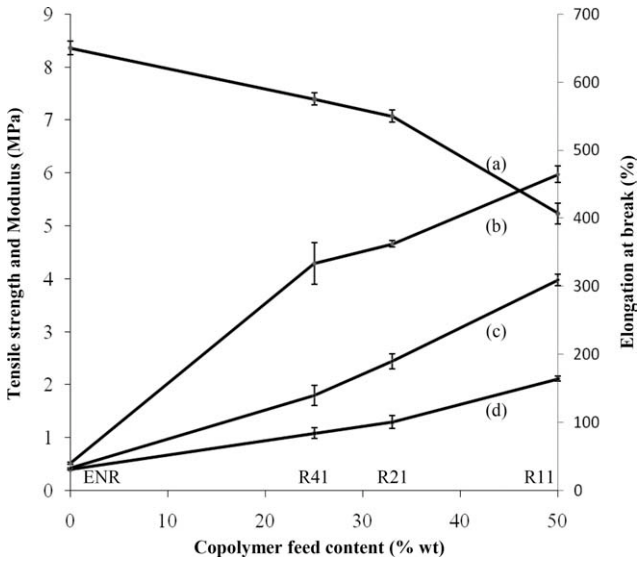

Figure 9 Elongation at break (a), Tensile strength (b), 100% Modulus, M100 (c), 300% Modulus, M300 (d) of ENR cured samples as a function of ENR20/copolymer feed content.

ENR in R11 also results in an enhancement of elongation at break.

Tensile properties of the cured samples as a function of ENR20/copolymer feed content are shown in Figure 9. The degree of improvement in tensile strength, M100, and M300 is dependent on the copolymer feed content, where R11 shows an improvement of more than 10 times of those of neat ENR20. This is due to the presence of network structure and "grafted" ENR chains, leading to a mobility restriction of the cured ENR products, as previously discussed. Additionally, the increase in the content of excess copolymers in the samples is also responsible for the increase in modulus and tensile strength. It is also clearly observed that elongation at break decreases with the increase in the copolymer content in the feed, mainly due to the increase in the content of excess copolymers. As the degree of improvement of tensile properties is strongly dependent on the ENR20/copolymer ratio in the feed, cured ENR products with specific properties can be obtained by adjusting this value. Given these excellent mechanical properties and their biocompatibility, the materials can be applied in various applications, especially in biomedical fields.

Permeability behaviors

Permeability characteristics of the cured samples are examined to elucidate their potential use in membrane applications. Theoretically, the permeability of a polymer for a gas penetrant is defined as a product of solubility coefficient and diffusion coefficient, where the former is derived from the relative size of penetrant and the inter/intrachain spacing of the polymer. The latter term is associated with sorption ability of the penetrant on the polymer.[36] Results of water vapor permeability of the cured samples, as summarized in Figure 10, show an increasing trend with increasing feed copolymer content, compared to that of neat ENR20, at 13 mm cc/(m^2·day atm). This is mainly because the cured products contain long-chain crosslink junctions that disrupt chain arrangement of the ENR matrix (See Fig. 1), leading to an enlargement of chain spacing and hence ease of water vapor permeation. EG sequences in the block copolymer also play a key role in the enhancement of the solubility coefficient term, as its strong hydrophilic nature provides high sorption ability to the vapor. This agrees with those observed by Zenkiewicz et al.[37] that the presence of 20% of PEG in the PLLA matrix doubly increased the water permeability of the mixture.

Results on oxygen permeability, as also shown in Figure 10, indicate that an increase in copolymer content in the cured materials leads to a drastic reduction in the oxygen permeability. Oxygen permeability of pristine ENR25, PEG and PLLA was reported as 328, 17, and 17 mm cc/(m^2 day atm), respectively.[36,38,39] Given the much lower values for PEG and PLA compared with that of ENR, a decrease in the permeability of the cured ENR samples is expected as a result from the incorporation of the copolymer. The reduction in the oxygen permeability can be explained in terms of a decrease in both diffusion and solubility coefficients, due to the relatively larger size of oxygen molecule and its nonpolar nature.

The variation in the oxygen permeability as a function of ENR20/copolymer content can be explained by the following empirical model, which was modified from that proposed by Paul et al. in the explanation of polymer blend characteristics.[40]

$$\log P_{cured} = \phi_{co} \log P_{co} + \phi_{ENR} \log P_{ENR} \qquad (4)$$

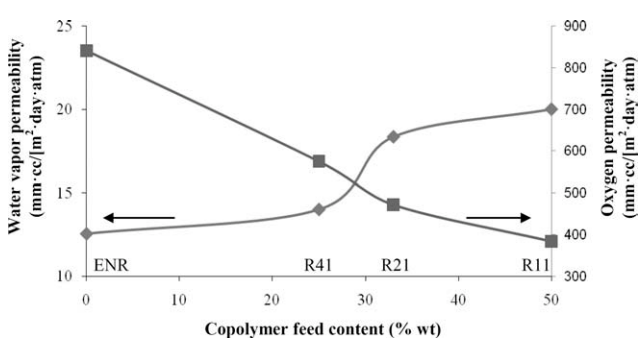

Figure 10 Water vapor and oxygen permeabilities of cured ENR samples as a function of ENR20/copolymer feed content.

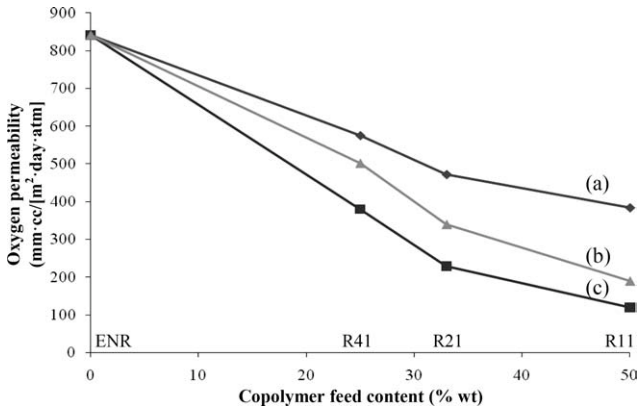

Figure 11 Experimental (a) and theoretical oxygen permeability: the free volume theory (b) and the empirical model (c), of cured samples as a function of ENR20/copolymer feed content.

where P_{cured} is gas permeability of the cured samples.

ϕ_{co} and ϕ_{ENR} are volume fractions of copolymer and ENR20 in the cured samples.

P_{co} and P_{ENR} are oxygen permeabilities of pure copolymer and ENR components.

Alternatively, the free volume model,[40] which is used to explain the transport behavior of gas in a polymer matrix, can be adopted, as described below:

$$\ln\frac{P_{cured}}{A} = \left[\frac{\phi_{ENR}}{\ln\left(\frac{P_{ENR}}{A}\right)} + \frac{\phi_{co}}{\ln\left(\frac{P_{co}}{A}\right)}\right]^{-1} \quad (5)$$

where A is parameter for free volume model at 25°C, 7.9×10^{-7} (cm^3(STP)·cm/[cm^2 sec cmHg])

Figure 11 summarizes oxygen permeability of the cured samples obtained from experiments, compared with those calculated from the empirical model and the free volume theory. Data obtained from the two models are significantly lower than the experimental results, probably because the models were designed for polymer blend systems. However, these cured ENR materials consist of full/partial crosslinked networks and blend mixtures. The free volume theory is a closer match to the experimental values, and perhaps more suitable to describe the gas permeability behavior of these materials. The higher experimental values compared to the predicted values by the free volume theory is probably due to the long-chain crosslink junctions derived from the block copolymers, which leads to formation of excess free volume in the cured network and hence, higher gas permeability.

Carbon dioxide permeability characteristics of ENR20 and R11 are compared in Table III. The values of 6142, 531, and 72 mm cc/(m^2 day atm) were reported for ENR25, PEG, and PLA, respectively.[38,39,41] Given the empirical model ($\log P_{cured} = \phi_{co}\log P_{co} + \phi_{ENR}\log P_{ENR}$), the CO_2 permeability of the cured samples is expected to decrease with increasing copolymer content. The experimental data, however, shows the reverse trend, where the cured R11 sample shows higher CO_2 permeability of more than two times, compared to that of the original ENR20. This intriguing behavior is mainly due to EG segments in the copolymer chains. It was reported that PEG can dissolve a substantial amount of sour gas.[42] Ether groups in PEG as polar moiety groups have affinity to CO_2 gas due to dipole-quadrupole interaction.[38] CO_2 is present as a strong sorbing penetrant for PEG, resulting in large solubility coefficient. The polymer matrix is subsequently plasticized by high concentration of this strong sorbing penetrant, resulting in an increase in local segment motion. Therefore, an enhancement in diffusion coefficients and permeability is achieved.[36,38,43] In addition, the presence of hydroxyl end-groups from "grafted" or "free" copolymers in the ENR matrix, and the newly formed hydroxyls from ring-opening reaction of epoxide (See Fig. 4), also favor the transport of CO_2 through the membrane because of its acidity.

TABLE III
Carbon Dioxide, Oxygen Permeability, and CO_2/O_2 Selectivity of ENR20 and Cured R11 Sample

Samples	CO_2 permeability (mm·cc/[m^2·day·atm])	O_2 permeability (mm·cc/[m^2·day·atm])	CO_2/O_2 selectivity
ENR20	6 117	841	7.3
R11	12 840	384	33.4

Results on CO_2/O_2 selectivity are also summarized in Table III. An enhancement in the CO_2/O_2 selectivity of more than four times is observed in R11 sample, compared with that of the neat ENR20. The ideal selectivity of penetrant is defined as the product of diffusivity selectivity and solubility selectivity. For rubbery polymer, it is commonly found that the selectivity is dominated by the solubility term.[36] This is firmly supported, as the solubility selectivity of the system strongly favors the transport of CO_2, as previously discussed. In addition, the permeability and selectivity of these materials may be further adjusted by varying the block length of EG sequence in the copolymer chains. Therefore, these copolymer-cured ENR samples are excellent choice for use as selective materials in membrane applications.

CONCLUSIONS

OH-capped LLA/EG/LLA triblock copolymer is used as a macromolecular crosslink agent for the ENR matrix by utilizing ring-opening reaction of epoxides and hydroxyl groups, using $Sn(Oct)_2$ as a

catalyst. ^{1}H-NMR and ATR-FTIR spectra indicate the formation of chemical bonds between copolymer chains and ENR. Efficiency of the crosslinked reaction is varied as a function of ENR/copolymer feed ratios, which is reflected by the content of "crosslinked," "grafted," and "free" simple blend fractions of the copolymer-cured ENR samples. These are examined by ^{1}H-NMR, ATR-FTIR, XRD, solvent fractionation, and swelling experiments. The cured ENR products exhibit drastic improvement in tensile properties, suitable for use as crosslinked rubber materials for specific and high-value applications. The use of a rather high content of the biocompatible/biodegradable copolymer as a curing agent is, therefore, not a major concern. Improvement in permeability and selectivity behaviors of the materials is also achieved, where water vapor and carbon dioxide permeability increase with an increase in copolymer feed content. The opposite trend is observed for oxygen permeability. These cured materials with excellent properties show high potential for use in biomedical and membrane applications. In addition, the properties of these cured materials can be fine tuned for specific applications by varying the ENR20/copolymer ratios, the epoxide content of ENR, and the relative block lengths of the copolymer.

References

1. Bhowmick, A. K.; Stephens, H. L. Handbook of Elastomers; Marcel Dekker: New York,2001.
2. Morgan, B.; McGill, W. J. J Appl Polym Sci 2000, 76, 1413.
3. Porter, M. J Appl Polym Sci 1967, 11, 2255.
4. Craig, D.; Davidson, W. L.; Juve, A. E.; Geib, I. G. J Polym Sci 1951, 6, 1.
5. Bristow, G. M.; Moore, C. G.; Russell, R. M. J Polym Sci Part A: General Papers 1965, 3, 3893.
6. Bristow, G. M. J Appl Polym Sci 1965, 9, 3255.
7. Moore, C. G.; Scanlan, J. J Polym Sci 1960, 43, 23.
8. Dunn, J. R. J Appl Polym Sci 1963, 7, 1543.
9. Chowdhury, R. J Appl Polym Sci 2007, 103, 1206.
10. Minoura, Y.; Asao, M. J Appl Polym Sci 1961, 5, 233.
11. Minoura, Y.; Asao, M. J Appl Polym Sci 1961, 5, 401.
12. Akiba, M.; Hashim, A. S. Prog Polym Sci 1997, 22, 475.
13. Gelling, I. R. J Natural Rubber Res 1991, 6, 184.
14. Hashim, A. S.; Kohjiya, S. J Polym Sci Part A: Polym Chem 1994, 32, 1149.
15. Gelling, I. R. Rubber Chem Technol 1985, 58, 86.
16. Perera, M. C. S. J Appl Polym Sci 1990, 39, 749.
17. Jayawardena, S.; Reyx, D.; Durand, D.; Pinazzi, C. P. Die Makromolekulare Chemie 1984, 185, 2089.
18. Derouet, D.; Radhakrishnan, N.; Brosse, J.-C. Boccaccio, G. J Appl Polym Sci 1994, 52, 1309.
19. Mohanty, S.; Nando, G. B.; Vijayan, K.; Neelakanthan, N. R. Polymer 1996, 37, 5387.
20. Derouet, D.; Brosse, J.-C.; Challioui, A. Eur Polym J 2001, 37, 1315.
21. Derouet, D.; Brosse, J.-C.; Challioui, A. Eur Polym J 2001, 37, 1327.
22. Gupta, A. P.; Kumar, V. Eur Polym J 2007, 43, 4053.
23. Cohn, D.; Younes, H. J Biomed Mater Res 1988, 22, 993.
24. Deng, X. M.; Xiong, C. D.; Cheng, L. M.; Xu, R. P. J Polym Sci Part C, Polym Lett 1990, 28, 411.
25. Kulkarni, R. K.; Moore, E. G.; Hegyeli, A. F.; Leonard, F. J Biomed Mater Res 1971, 5, 169.
26. Saito, T.; Klinklai, W.; Yamamoto, Y.; Kawahara, S.; Isono, Y.; Ohtake, Y. J Appl Polym Sci 2009, 115, 3598.
27. Nghia, P. T.; Siripitakchai, N.; Klinklai, W.; Saito, T.; Yamamoto, Y.; Kawahara, S. J Appl Polym Sci 2008, 108, 393.
28. Nguyen, T.-H.; Petchsuk, A.; Tangboriboonrat, P.; Opaprakasit, M.; Sharp, A.; Opaprakasit, P. Adv Mater Res 93 2010, 94, 198.
29. Saendee, P.; Tangboriboonrat, P. Colloid Polym Sci 2006, 284, 634.
30. Derouet, D.; Tran, Q. N.; Thuc, H. H. J Appl Polym Sci 2009, 114, 2149.
31. Phinyocheep, P.; Phetphaisit, C. W.; Derouet, D.; Campistron, I.; Brosse, J. C. J Appl Polym Sci 2005, 95, 6.
32. Aprem, A. S.; Joseph, K.; Mathew, T.; Altstaedt, V.; Thomas, S. Eur Polym J 2003, 39, 1451.
33. Saito, T.; Klinklai, W.; Kawahara, S. Polymer 2007, 48, 750.
34. Mathew, V.; Sinturel, C.; George, S.; Thomas, S. J Mater Sci 45, 1769.
35. Yong, M. K.; Ismail, H.; Ariff, Z. M. Polym-Plast Technol Eng 2007, 46, 1001.
36. Johnson, T.; Thomas, S. Polymer 1999, 40, 3223.
37. Zenkiewicz, M.; Richert, J. Polym Test 2008, 27, 835.
38. Lin, H.; Freeman, B. D. J Membr Sci 2004, 239, 105.
39. Bao, L.; Dorgan, J. R.; Knauss, D.; Hait, S.; Oliveira, N. S.; Maruccho, I. M. J Membr Sci 2006, 285, 166.
40. Paul, D. R. J Membr Sci 1984, 18, 75.
41. Barrie, J. A.; Becht, M.; Campbell, D. S. Polymer 1992, 33, 2450.
42. Kuehne, D. L.; Friedlander, S. K. Indust Eng Chem Proc Des Dev 1980, 19, 609.
43. Koros, W. J.; Hellums, M. W. Fluid Phase Equilibria 1989, 53, 339.